Interpretation of the vibrational relaxation of H_2 in H_2 within the semiclassical effective mass approach

E. I. Dashevskaya, I. Litvin, and E. E. Nikitin
Schulich Faculty of Chemistry, Technion-Israel Institute of Technology, Haifa 32000, Israel and Max-Planck-Institut für Biophysikalische Chemie, Am Fassberg, D-37077 Göttingen, Germany

J. Troe
Max-Planck-Institut für Biophysikalische Chemie, Am Fassberg, D-37077 Göttingen, Germany and Institut für Physikalische Chemie, Universität Göttingen, Tammannstrasse 6, D-37077 Göttingen, Germany

(Received 15 May 2007; accepted 3 July 2007; published online 21 September 2007)

The temperature dependence of the rate coefficients for vibrational relaxation of H_2 in neat H_2 is interpreted within the semiclassical effective mass approach. Across the temperature range of 80–3000 K, the experimental rate coefficients vary by five orders of magnitude and fall onto a strongly nonlinear Landau-Teller plot. This behavior is explained by the nonclassical nature of the energy release and by a substantial participation of rotation of the colliding partners in inducing the vibrational transition. A single fitting parameter, the optimal reduced mass, permits one to represent the temperature dependence of the rate coefficient within a factor of 2. This parameter is found to be close to that obtained from a simple model suggested by Sewell *et al.* [J. Chem. Phys. **99**, 2567 (1993)]. © *2007 American Institute of Physics*. [DOI: 10.1063/1.2766949]

I. INTRODUCTION

Vibrational relaxation rates today can be determined accurately using close-coupling scattering methods whenever accurate interaction potentials are available from *ab initio* calculations. Besides being numerically not trivial, these calculations generally are not as transparent as one would like them to "understand" the phenomenon. For this reason, approximate simpler methods also find their justification when they lead to a rational interpretation of the experimental observables. One of these methods is the effective mass (EM) approach. This method for the calculation of vibrational relaxation rates of diatomic molecules in an atomic heat bath was formulated quite some time ago,[1] described in detail in the textbook[2] and applied, in a more sophisticated version, to specific systems in a number of articles (see, e.g., Refs. 3 and 4 and work cited therein). The method provides an approximate way to account for the effect of rotation on the vibrational energy transfer. At sufficiently high temperatures, the EM approach can be cast into the standard form of the Schwartz-Slawsky-Herzfeld (SSH) formalism,[5,6] within which the rate coefficient is represented as the leading Landau-Teller (LT) exponential term [called common trajectory (CT) approximation in Ref. 7] and its first quantum correction [corrected common trajectory (CCT) approximation[7]]. It was argued in Ref. 7 that the CCT approximation can also be applied to an arbitrary, not necessary repulsive, exponential interaction, such as was employed within the SSH theory. In this way it became possible to pass from a purely repulsive interaction to an attractive interaction which is of importance for lower temperatures. At present, the rate coefficients at the CT level, which is equivalent to linear response theory with a classical correlation function for the vibrational-thermal bath mode coupling, are documented for different types of interaction[8,9] such that the CCT generalization is straightforward. However, the passage to lower temperatures within the CCT approximation soon reaches its limits, i.e., the requirement that the energy transfer ΔE should be smaller than the initial E_i and final E_f collision energies, or, that, on average, the first quantum correction in the exponent (being proportional to T^{-1}) should be noticeably smaller than the leading LT-like term (being approximately proportional to $T^{-1/3}$). Then the CCT approximation should be replaced by a more general semiclassical (SC) approximation within which the condition $\Delta E \ll E_i, E_f$ is relaxed but both states are assumed to comply with the WKB conditions.[7] Recently, we have presented the EM version of the SC approximation for the temperature dependence of the vibrational relaxation rate coefficient of $N_2(v=1)$ in He (see Ref. 10) employing a realistic interaction potential. For this system, the effective mass μ_{EM} turned out to be quite close to the reduced mass μ of the N_2–He pair such that the effect of rotation was quite modest. In the present work we intend to treat a system where this is not the case.

The effective mass μ_{EM} is expected to deviate noticeably from μ for systems with higher interaction anisotropy and with higher ratio of μ to the reduced mass M of the diatom. A system that satisfies this condition is a hydrogen hydride-noble gas pair when μ_{EM} is considerably lower than μ.[1–4] For homonuclear diatomics, when the anisotropy is not very large and μ does not strongly exceed M, the effective mass μ_{EM} does not differ much from μ. However, this fact does not imply that the effect of rotation of the diatom on the vibrational relaxation is small since the relaxation rate depends exponentially on the effective mass. An example of such a case is provided by the relaxation of H_2 in He, a system with the most simple and well studied interaction potential. For the past decade, a number of theoretical papers were devoted to the vibrational relaxation of H_2 in He.[11–18]

In particular, the question of the participation of rotation of H_2 in the vibrational relaxation was addressed in detail. The high accuracy of quantum scattering calculations for atom-diatom system allowed one to thoroughly investigate the effect of anisotropy on the vibrational relaxation rate in a comparative study of two potential energy surfaces in conjunction with existing experimental data.[19] In anticipation of implementation of a similar program for more complicated collision systems, we consider here an another example of practical importance, the vibrational relaxation of H_2 in neat H_2

$$H_2(v=1)+H_2(v=0)\rightarrow H_2(v=0)+H_2(v=0). \tag{1}$$

The dynamics of H_2-H_2 collisions is quite complicated due to the contribution of the relative translation and two rotational modes to the vibrational deactivation of H_2. Earlier calculations[20–23] of the rate of the inelastic process (1) either completely ignored the effect of rotation[20] or introduced, for a given potential surface, severe dynamical simplifications[21–23] which still required extensive numerical work. It appears therefore of interest to see whether an analytical SC approach within the EM method can provide a physically reasonable interpretation of the temperature dependence of the vibrational relaxation of H_2 in neat H_2 gas which was measured by different techniques[24–27] over a wide temperature range from 3000 down to 50 K. In this paper, similar to our earlier approach,[10] we consider only the direct mechanism of vibrational relaxation which proceeds without the formation of a transient complex formed as a result of the translation-rotational energy exchange. The reason for this is twofold: first, the complex formation is expected to be unimportant for the collision energies exceeding the depth of the interaction potential, and, second, for the complex-assisted vibrational relaxation the temperature dependence of the rate coefficient shows upturn behavior which is not seen in the existing experimental data at lower temperatures.

This paper reports an analysis of the temperature dependence of the relaxation rate within a simplified version of the EM method, the optimal effective mass (OEM) approximation, using information from sections of the *ab initio* potential surface of the H_2-H_2 system. We ask the question which dynamical information can be obtained from the analysis of the Landau-Teller plot of the rate coefficient provided that the interaction potential is known reasonably well. The consistency of the analysis is checked by verifying the conditions of applicability of the OEM and WKB approximations to the rotation of H_2. The plan of the article is the following. Section II describes the SC-EM model and its SC-OEM extension and presents calculated encounter times for selected sections of the potential for H_2-H_2 system. Section III discusses SC rate coefficients within the breathing sphere model. The theoretical temperature dependence of the SC-OEM rate coefficients in Sec. IV is compared with the experimental data. The fitted value of the OEM is shown to be compatible with estimates for simple model potentials and the OEM approach is checked for internal consistency. Finally, Sec. V summarizes our findings.

II. THE SEMICLASSICAL EFFECTIVE MASS MODEL

The OEM model for collisions of two diatomic molecules is based on the generalization of a similar model for atom-diatom collisions. In turn, the OEM model for the latter system is a specific limiting case of the EM model. We, therefore, first consider the EM model for atom-diatom collisions such as described in Refs. 1–4. Here the model introduces a single "driving mode" q in localized regions of the potential, being embedded into the two-dimensional space of the radial variable R (the distance between the atom and the center of mass of the diatom) and the angular coordinate γ (the angle between the vector R and the molecular axis). The driving mode is a specific combination of the coordinate displacements ΔR and $\Delta\gamma$ which describes the motion along the gradient of the atom-rigid rotor interaction potential $U(R;\gamma)$ in a small region centered at R^*,γ^*. The two-dimensional potential $U(R^*+\Delta R;\gamma^*+\Delta\gamma)$ is then replaced by a one-dimensional potential $U_{\mathrm{EM}}(q;R^*,\gamma^*)$ and the reduced mass μ is changed into the effective mass μ_{EM} which depends on μ, the moment of inertia of the diatom I, and the contour line of the potential $U(R,\gamma)$ for a given total energy (see Refs. 1–4). Within the EM method, the translational and rotational degrees of freedom are treated on the same footing. Their relative importance is hidden in the definition of the driving mode, and the energy released as a result of vibrational deactivation is distributed among translational and rotational modes. The EM method does not address the question about this distribution.

Due to the steep R dependence of the interaction, the inverse dependence of the contour lines on the energy is weak in the energy range of interest, such that one can ignore it altogether. Then, μ_{EM} and U_{EM} can be parametrized only through γ^*, i.e., $\mu_{\mathrm{EM}}=\mu_{\mathrm{EM}}(\gamma^*)$ and $U^{\mathrm{EM}}=U^{\mathrm{EM}}(q,\gamma^*)$. Typically, $\mu_{\mathrm{EM}}=\mu_{\mathrm{EM}}(\gamma^*)$ passes through a minimum (or minima), reaching its maximum $\mu_{\mathrm{EM}}=\mu$ for linear arrangements.

The EM encounter time $\tau_{\mathrm{EM}}(E,\gamma^*)$ is defined as the integral

$$\tau_{\mathrm{EM}}(E,\gamma^*)=\int_{q_s}^{q_t(\gamma^*)}\frac{\sqrt{\mu_{\mathrm{EM}}(\gamma^*)}dq}{\sqrt{2(U_{\mathrm{EM}}(q,\gamma^*)-E)}}, \tag{2}$$

in which E is the energy of the driving mode, $q_t(\gamma^*)$ is the turning point, and q_s is a point in the classically forbidden region of motion at which the integral can be regarded as converged. The SC expression for the rate coefficient finally assumes the form

$$k_{10}^{\mathrm{SC\text{-}EM}}(T)=\sqrt{\frac{8kT}{\pi\mu}}\int_0^{\pi}A(\gamma^*)2\pi R^2(\gamma^*)\sin\gamma^*d\gamma^*\times\int_0^{\infty}\exp\left(-\frac{2}{\hbar}\int_{E_i}^{E_i+\hbar\omega}\tau_{\mathrm{EM}}(E,\gamma^*)dE-E_i/kT\right)\frac{dE_i}{kT}. \tag{3}$$

In this expression the integration over E is related to the recovery of the Landau semiclassical exponent from the classical encounter time,[7] the integration over E_i to the canonical averaging of the transition probability over the initial energy of the driving mode, and the integration over γ^* to the scan-

ning of the mean transition probability across the dividing surface with the surface element $dS^*=2\pi R^2(\gamma^*)\sin\gamma^* d\gamma^*$. The factor $A(\gamma^*)$ does not depend on the temperature for an exponential repulsion and it is assumed to depend only weakly on T for other types of steep interactions. In this way, Eq. (3) yields the analytical temperature dependence (though in integral form) of the SC-EM rate coefficient if the dependences of A and τ on γ^* are known.

Simplified versions of Eq. (3) can be obtained to correspond to different limiting types of the dependence of the encounter time on γ^*. If the dependence is completely neglected, the double integral in Eq. (3) is factored into two integrals such that the SC-EM approach becomes equivalent to the SC breathing sphere (BS) model

$$k_{10}^{\text{SC-BS}}(T) \propto T^{1/2}\int_0^\infty \exp\left(-\frac{2}{\hbar}\int_{E_i}^{E_i+\hbar\omega}\tau_{\text{BS}}(E)dE - E_i/kT\right)\frac{dE_i}{kT}. \tag{4}$$

If the γ^* dependence of the encounter time is so strong that only a relatively small integration region $\Delta\gamma^*$ around a certain value of $\gamma^*=\gamma^\dagger$ contributes to the integral over γ^*, the integral can be calculated in the steepest descent (SD) approximation. This yields the OEM approximation

$$k_{10}^{\text{SC-OEM}}(T) \propto T^{1/2}\int_0^\infty \Delta\gamma^*(E_i) \times\exp\left(-\frac{2}{\hbar}\int_{E_i}^{E_i+\hbar\omega}\tau^\dagger(E)dE - E_i/kT\right)\frac{dE_i}{kT}, \tag{5}$$

where

$$\Delta\gamma^*(E_i)=\sqrt{\pi}\left(\frac{1}{\hbar}\int_{E_i}^{E_i+\hbar\omega}(d^2\tau_{\text{EM}}(E,\gamma^*)/d\gamma^{*2})_{\gamma^*=\gamma^\dagger}dE\right)^{-1/2} \tag{6}$$

and where $\tau^\dagger(E)$ is the minimal value of $\tau_{\text{EM}}(E,\gamma^*)$ attained at $\gamma^*=\gamma^\dagger$.

The main difference in the temperature dependences of the rate coefficients from Eqs. (4) and (5) is due to the different exponents containing τ_{BS} and $\tau^\dagger(E)$. The factor $\Delta\gamma^*(E_i)$ in Eq. (5) introduces only a small correction to Eq. (4). The nature of this correction can be easily understood in the high-temperature limit (CCT approximation) for an angle-independent exponentially repulsive potential of slope α. In this limit, Eq. (4) becomes the standard SSH expression

$$k_{10}^{\text{SC-BS}}(T) \to k_{10}^{\text{CCT-BS}}(T) \equiv k_{10}^{\text{SSH}}(T) \propto T^{1/3}\exp(-3(T_{\text{LT}}/T)^{1/3}+\hbar\omega/2kT), \tag{7}$$

with $T_{\text{LT}}=\pi^2\omega^2\mu/2k\alpha^2$. On the other hand, Eq. (5) yields

$$k_{10}^{\text{SC-OEM}}(T) \to k_{10}^{\text{CCT-OEM}}(T) \propto T^{1/2}\exp(-3(T_{\text{LT}}^\dagger/T)^{1/3} + \hbar\omega/2kT), \tag{8}$$

with $T_{\text{LT}}^\dagger=\pi^2\omega^2\mu^\dagger/2k\alpha^2$. The main difference in the temperature dependences of Eqs. (7) and (8) arises from different values of the LT temperatures, T_{LT} and $T_{\text{LT}}^\dagger$. The difference in the preexponential factors of Eqs. (7) and (8) is hardly noticeable unless the values of T_{LT} and $T_{\text{LT}}^\dagger$ are known with high accuracy.

In our recent work on the N_2–He relaxation of N_2 in He (see Ref. 10), we have used two SC expressions which were similar to Eq. (8), with angle-independent masses μ and $\mu^\dagger$ which allowed us to provide upper and lower bounds for $k_{10}^{\text{SC-EM}}$, i.e., $k_{10,\max}^{\text{SC}}=k_{10}^{\text{SC-EM}}|_{\mu_{\text{EM}}=\mu^\dagger}$ and $k_{10,\min}^{\text{SC}}=k_{10}^{\text{SC-EM}}|_{\mu_{\text{EM}}=\mu}$. The ratio of two bounds, $k_{10,\max}^{\text{SC}}/k_{10,\min}^{\text{SC}}$, as obtained from the high-temperature limits, Eqs. (7) and (8), is about

$$k_{10,\max}^{\text{SC}}/k_{10,\min}^{\text{SC}} \approx \exp\left(\frac{2(\mu-\mu^\dagger)}{\mu}\left(\frac{T_{\text{LT}}}{T}\right)^{1/3}\right). \tag{9}$$

Equation (9) provides useful bounds for the estimation of $k_{10}^{\text{SC-EM}}$ when the difference $\mu-\mu^\dagger$ is small enough such that the exponent in Eq. (9) is not noticeably larger than unity. This was the case for N_2–He collisions.[10] If the difference $\mu-\mu^\dagger$ is not small such that the exponential in the right-hand side of Eq. (9) is large, the above estimate loses its meaning, and the OEM approximation has to be used instead.

The OEM approximation of Eq. (3), with the additional assumption that the dependence of τ on γ^* is governed mainly by the factor $\sqrt{\mu_{\text{EM}}(\gamma^*)}$, yields

$$k_{10}^{\text{SC-OEM}}(T) \propto T^{1/2}\int_0^\infty\left(\frac{2}{\hbar}\int_{E_i}^{E_i+\hbar\omega}\tau^\dagger(E)dE\right)^{-1/2} \times\exp\left(-\frac{2}{\hbar}\int_{E_i}^{E_i+\hbar\omega}\tau^\dagger(E)dE - E_i/kT\right)\frac{dE_i}{kT}, \tag{10}$$

where $\tau^\dagger(E)=\tau_{\text{EM}}(E,\gamma^\dagger)$. Since the integration over the angles is not present in Eq. (10), it directly yields the temperature dependence of the rate coefficient under the condition that the energy dependence of $\tau^\dagger$ is known.

Equation (10) suggests a simple generalization for the case of diatom-diatom collisions. In this case, instead of a single angular variable γ^*, there are three variables: the angle γ_1^* between the axis $\mathbf{n}_1$ of the first diatom and the collision axis $\mathbf{R}$, the angle γ_2^* between $\mathbf{n}_2$ and $\mathbf{R}$, and the dihedral angle ϕ_{12}^* between the planes formed by the vectors $\mathbf{n}_1$, $\mathbf{R}$ and $\mathbf{n}_2$, $\mathbf{R}$. If a minimum of $\mu_{\text{EM}}=\mu_{\text{EM}}(\gamma_1^*,\gamma_2^*,\phi_{12}^*)$ exists with respect to all three angles, such that $\mu^\dagger=\mu_{\text{EM}}(\gamma_1^\dagger,\gamma_2^\dagger,\phi_{12}^\dagger)$, and the steepest descent approximation is applied to all three, the expression for $k_{10}^{\text{SC-OEM}}(T)$ assumes the form

$$k_{10}^{\text{SC-OEM}}(T) = CT^{1/2}\int_0^\infty\left(\frac{2}{\hbar}\int_{E_i}^{E_i+\hbar\omega}\tau^\dagger(E)dE\right)^{-3/2} \times\exp\left(-\frac{2}{\hbar}\int_{E_i}^{E_i+\hbar\omega}\tau^\dagger(E)dE - E_i/kT\right)\frac{dE_i}{kT}. \tag{11}$$

In the following, Eq. (11) will be used for an approximate analysis of the temperature dependence of process (1). The key quantity to be considered is the encounter time $\tau^\dagger(E)$, and its calculation requires information at least on some sec-

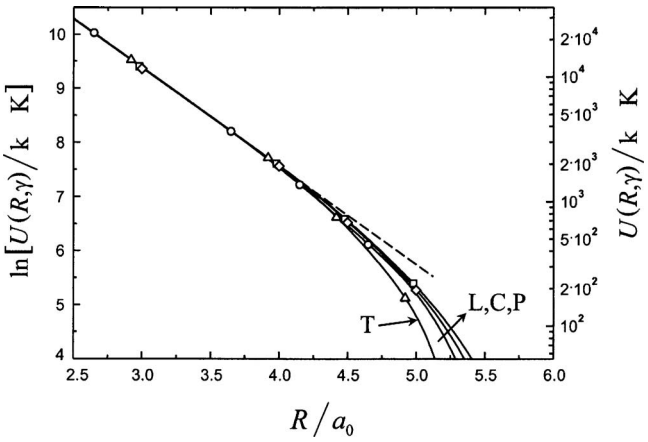

FIG. 1. Shifted interaction potentials in four sections of the PES for the H_2-H_2 system as a function of the distance R between molecular centers of mass. Configurations are crossed (C), nonshifted; parallel (P), shifted by $0.02a_0$; linear (L), shifted by $0.35a_0$; and T-shaped (T), shifted by $0.08a_0$ (after Ref. 28).

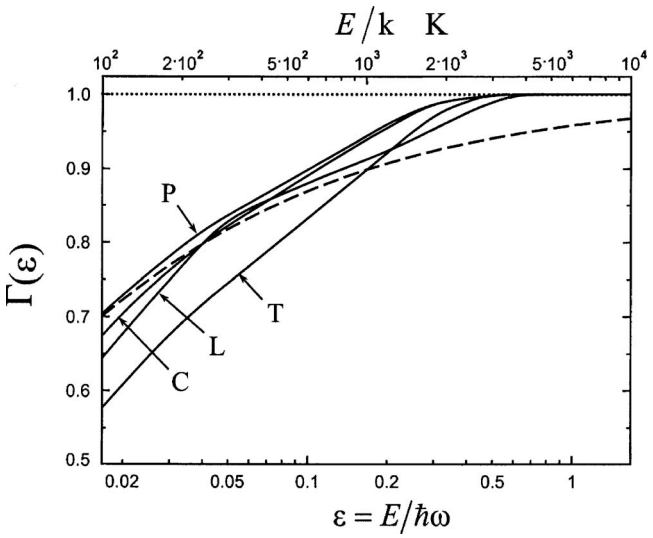

FIG. 2. Ratio $\Gamma(\varepsilon)$ of the encounter times to the high-energy encounter time vs reduced energy $\varepsilon=E/\hbar\omega$ and the "temperature" E/k for four configurations. The dotted horizontal line shows the high-energy asymptote; the dashed line corresponds to the Morse potential with the well depth equal to that for the parallel configuration.

tions of the potential energy surface (PES). It is clear from the above discussion that the nonempirical determination of OEM requires the search of a minimum of EM on the multidimensional PES. We avoid this numerical procedure by considering OEM as a fitting parameter, the optimal value of which is substantiated by estimate for a reasonably simple model (see Sec. IV). We also reiterate here that the value of the factor C in Eq. (11) depends critically on the strength of the vibrational-rotational translational coupling, but it does not affect the temperature dependence of the rate coefficient.[10] We therefore regard C, in our discussion of the temperature dependence of the relaxation rate, as yet another fitting parameter.

Among several *ab initio* calculation of PES for the H_2-H_2 system[29–31] we have chosen Ref. 29 which most directly provides the information that we need in our approach. In particular, we consider sections of the PES that correspond to linear (L, $\gamma_1^*=0$, $\gamma_2^*=0$, ϕ_{12}^* arbitrary), crossed (C, $\gamma_1^*=\pi/2$, $\gamma_2^*=\pi/2$, $\phi_{12}^*=\pi/2$), parallel (P, $\gamma_1^*=\pi/2$, $\gamma_2^*=\pi/2$, $\phi_{12}^*=0$), and T-shaped (T, $\gamma_1^*=0$, $\gamma_2^*=\pi/2$, ϕ_{12}^* =arbitrary) configurations of the H_2-H_2 complex as functions of the distance R between the centers of mass of the two H_2 molecules. It follows from symmetry considerations that the driving mode is R and that the effective mass in the selected configurations is equal to the reduced mass of the partners, $\mu_{\mathrm{EM}}^{\mathrm{L}}=\mu_{\mathrm{EM}}^{\mathrm{C}}=\mu_{\mathrm{EM}}^{\mathrm{P}}=\mu_{\mathrm{EM}}^{\mathrm{T}}=\mu$. Following the analysis of our previous work[10] we constructed the logarithmic plots of four potentials $U^X(R)$ (X=L,C,P,T). Shifting these potentials along the R axis, Fig. 1 demonstrates their nearly identical exponential dependence on R at high energies. Since the encounter time does not depend on such shifts, the data presented in Fig. 1 are sufficient for calculations of encounter times $\tau_{\mathrm{EM}}^X(E)$ for all four configurations. Inspection of Fig. 1 shows that all shifted potentials at high energies are superimposed on each other and are well approximated by an exponential dependence on αR with a slope of α =1.815 a.u. Therefore, the high-energy encounter times $\tau_{\mathrm{high}}^X(E)$ are the same for all X and are given by

$$\tau_{\mathrm{high}}^X(E)=\tau_{\mathrm{high}}(E)=\pi\sqrt{\mu}/\alpha\sqrt{2E}. \tag{12}$$

At lower energies, the shifted potentials differ from each other and this difference is reflected by different encounter times. This is illustrated in Fig. 2 where the ratios $\Gamma^X(E)$ $=\tau^X(E)/\tau_{\mathrm{high}}(E)$ are plotted as functions of the energy. The upper (Γ_{P}) and the lower (Γ_{T}) values of this ratio can be used for estimation of the lower and the upper bounds of the rate coefficient.

III. SEMICLASSICAL RATE COEFFICIENTS FOR BREATHING SPHERE MODEL

One of the earliest calculations of vibrational relaxation rates of H_2 in H_2 by Calvert[20] was accomplished within the quantum BS model with a Morse interaction potential

$$U^M(R)=D^M[\exp(-\alpha^M(R-R_e)) - 2\exp(-\alpha^M(R-R_e)/2)]. \tag{13}$$

The parameters of this potential were chosen such that the high-energy slope of the repulsive part of the potential was α^M=1.832 a.u. and the well depth D^M/k=132 K. It was found that the derived theoretical rate coefficient roughly corresponded to the experimental data available at that time. This led to the conclusion that rotation of H_2 presumably does not play any significant role in the vibrational deactivation. In order to further investigate this conclusion, we have performed SC-BS calculations for both the Morse and *ab initio* potentials. The calculation of the rate coefficients for a Morse potential is simplified by the fact that the encounter time τ^M and the SC exponent for a Morse potential can be expressed analytically. They are[32,33]

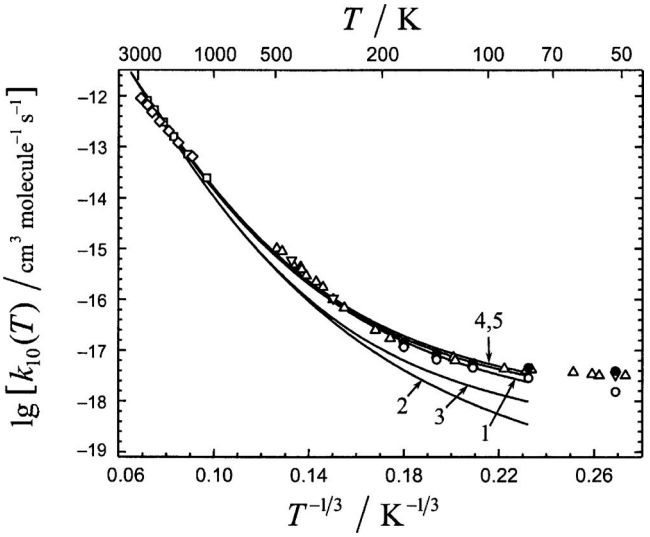

FIG. 3. Comparison of the LT plots for the SC-BS rate coefficients with experimental data (after Huestis, Ref. 34). Shock tube experiments: □ (Ref. 24), ◇ (Ref. 25); laser Raman excitation and detection experiments: △ normal-H_2 (Ref. 26); ● ortho-H_2, ○ para-H_2, and ▽ normal-H_2 (Ref. 27). Curve 1 corresponds to the Morse potential with *ab initio* parameters, curve 2 to a purely repulsive potential, curve 3 to an *ab initio* potential with $\mu_{EM}=\mu=1$, and curves 4 and 5 to an *ab initio* potential with fitted effective masses μ_{EM} equal to 0.849 and 0.833, respectively. The curves are terminated at 80 K to indicate that, for lower temperatures, the relaxation via the complex formation may become efficient.

$$\tau^M(E)=\frac{2\sqrt{\mu}}{\alpha^M\sqrt{2E}}\arctan\left(\sqrt{\frac{E}{D^M}}\right),$$

$$\int^E \tau^M(E)dE=\frac{2\sqrt{\mu}}{\alpha^M}\left[\sqrt{2E}\arctan\sqrt{E/D^M}-\sqrt{D^M/2}\times\ln(1+E/D^M)\right]. \tag{14}$$

In our calculations, we have used the high-energy slope parameters $\alpha^M=\alpha=1.815$ a.u. and the well depths $D_P^M/k=26$ K and $D_T^M/k=78$ K as given for the *ab initio* potential in P and T configurations. We note that the above value of α^M is very close to that of Calvert ($\alpha^M=1.832$ a.u.) but the wells are much shallower. The calculated LT plot of the Morse SC-BS rate coefficient $k_{10}^{\text{MSC-BS}}$ with the given values of parameters α^M and D_P^M is represented in Fig. 3 by curve 1. Once again one can conclude that the BS model with the Morse potential satisfactorily reproduces the temperature dependence of the experimental rate coefficient, this time for a wider temperature range compared to that discussed by Calvert. The importance of the attraction is demonstrated by the comparison with curve 2 which corresponds to a purely repulsive interaction. For both cases, the LT temperature is 3.12×10^5 K.

Calculations of the rate coefficient $k_{10}^{\text{SC-BS}}$ for the *ab initio* potential $U_P(R)$ are presented by curve 3 which falls noticeably below both the experimental data at medium to low temperatures and the theoretical values for the Morse interaction. The reason for this discrepancy is best understood by comparing encounter times for the Morse and *ab initio* potentials, see Fig. 2. At low and high energies τ^M and τ^P are very close, while over the intermediate energy range that contributes most to the SC exponent, τ^M is smaller than τ^P, thus, making $k_{10}^{\text{MSC-BS}}$ larger than $k_{10}^{\text{SC-BS}}$. By comparing curves 3 and 1 in Fig. 3, the former calculated for the *ab initio* potential and the latter for the Morse potential, we conclude that the use of the Morse potential is inappropriate and that the agreement of $k_{10}^{\text{MSC-BS}}$ with experimental data is misleading and the result of error compensation, see below. Similar conclusions are obtained from the calculations for the T configuration.

The failure of the BS model, employing the *ab initio* potentials, to reproduce the experimental results has to be attributed to the fundamental shortcoming of this model, namely, to the neglect of the effect of molecular rotation on vibrational energy transfer. An indication for the importance of the rotation can already be inferred by the possibility of fitting the BS curve to the experimental points in replacing the reduced mass of the colliding partners μ by a certain effective mass μ_{EM}. Though this procedure is not consistent with the BS concept, it works in the direction of the effective mass approach. The result of such fitting is shown by curves 4 and 5 that correspond to two values of the ratio μ_{EM}/μ equal to 0.849 and 0.833, respectively. The qualitative agreement of the fitted curves of the BS model with the experimental data calls for a more consistent EM approach such as outlined in Sec. II and elaborated in the following.

IV. SEMICLASSICAL RATE COEFFICIENTS FOR THE OPTIMAL EFFECTIVE MASS MODEL

Following the discussion in Secs. II and III, we reformulate the temperature dependence of the SC-OEM rate coefficient in the form

$$k_{10}^{\text{SC-OEM}}(T,T_{\text{LT}}^{\dagger})=C\sqrt{\frac{T}{T_{\text{vib}}}}\int_0^{\infty}\left(2\sqrt{\frac{T_{\text{LT}}^{\dagger}}{T_{\text{vib}}}}\int_{\varepsilon_i}^{\varepsilon_i+1}\Gamma^{\dagger}(\varepsilon)\varepsilon^{-1/2}d\varepsilon\right)^{-3/2}\times\exp\left(-2\sqrt{\frac{T_{\text{LT}}^{\dagger}}{T_{\text{vib}}}}\int_{\varepsilon_i}^{\varepsilon_i+1}\Gamma^{\dagger}(\varepsilon)\varepsilon^{-1/2}d\varepsilon-\frac{T_{\text{vib}}}{T}\varepsilon_i\right)\frac{T_{\text{vib}}}{T}d\varepsilon_i, \tag{15}$$

where C is a temperature-independent factor, $\varepsilon=E/\hbar\omega$, $\varepsilon_i=E_i/\hbar\omega$, $T_{\text{vib}}=\hbar\omega/k$, $T_{\text{LT}}^{\dagger}=\pi^2\omega^2\mu^{\dagger}/2k\alpha^2$, and $\Gamma^{\dagger}(\varepsilon)$ is the ratio of the encounter time to the high-energy encounter time in the optimal configuration. Since the latter is not known, we have used two ratios, $\Gamma^{\text{P}}(\varepsilon)$ and $\Gamma^{\text{T}}(\varepsilon)$ such as presented in Fig. 2 which are expected to bracket $\Gamma^{\dagger}(\varepsilon)$. The only fitting parameter, besides the constant factor C, is the OEM $\mu^{\dagger}$ that enters the optimal LT temperature.

The best fit of the LT plot, $\log(k_{10}^{\text{SC-OEM}})$ vs $T^{-1/3}$, with $\Gamma^{\dagger}(\varepsilon)=\Gamma^{\text{P}}(\varepsilon)$ to the experimental data in the range $70<T<3000$ K, is shown in Fig. 4. The optimal fit parameter, $(\mu^{\dagger}/\mu)_{\text{P}}$, was found to be 0.681 ± 0.008, with $C=6.0\times10^{-6}$ cm^3 molecule^{-1} s^{-1}. For the same value of $\mu^{\dagger}/\mu$, plots of $\log(k_{10}^{\text{SC-OEM}})$ are also shown for $\Gamma^{\dagger}(\varepsilon)=1$ (pure exponential repulsion, dashed line), for $\log(k_{10}^{\text{CCT-OEM}})$ (SSH-like approximation, upper dotted curve), and for $\log(k_{10}^{\text{CT-OEM}})$ (LT-like approximation, lower dotted curve). The three latter curves illustrate the effect of attraction, the

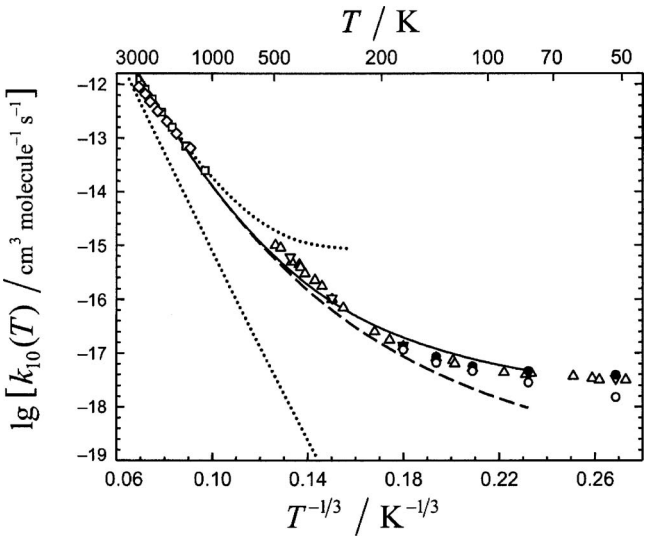

FIG. 4. Comparison of the LT plots for the SC-OEM rate coefficients (full curve, potential for P configuration, μ=0.68) with experimental data (see Fig. 3). The dashed curve corresponds to SC-OEM rate coefficient for pure repulsive interaction, and the two dotted curves represent the OEM rate coefficients calculated in the common trajectory approximation (CT, the LT approximation with OEM) and corrected common trajectory approximation (CCT, the SSH approximation with OEM). The curves are terminated at 80 K to indicate that, for lower temperatures, the relaxation via the complex formation may become efficient.

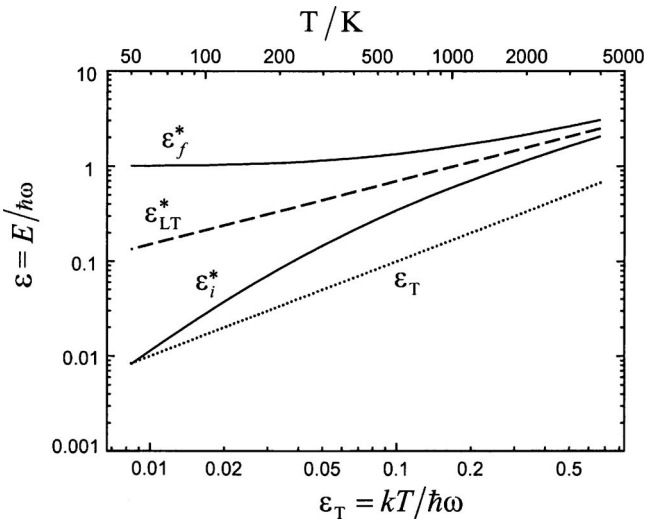

FIG. 5. Interpretation of the steepest descent approximation for SC vibrational relaxation: SD energy for the initial state $\varepsilon_i^*=E_i^*/\hbar\omega$, SD energy for the final state $\varepsilon_f^*=\varepsilon_i^*+1$, and SD energy for the LT treatment $\varepsilon_{\mathrm{LT}}^*=T_{\mathrm{LT}}/\hbar\omega$ vs temperature $\varepsilon_T=kT/\hbar\omega$.

performance of the first quantum correction, and the complete failure of the LT description, respectively.

It is of interest to provide a qualitative interpretation of the value of the optimal mass found from the best fit of the SC-OEM rate coefficient to the experiments. To this end, in a rough approximation, we consider one of the colliding molecules to be a structureless particle, and we use the expression for the EM for the collision of a diatom with an atom such as suggested in Ref. 3 [see Eq. (4) of Ref. 3],

$$\mu_{\mathrm{EM}}(\gamma^*)=\mu I/(I+\mu r^2\sin^2\theta), \tag{16}$$

where r is half the equilibrium internuclear distance of the diatom r_e, I is the moment of inertia of H_2, and $\theta=\theta(\gamma^*)$ is the angle between the molecular axis and the line connecting the H atom of one H_2 molecule with the center of the other. The function $\theta=\theta(\gamma^*)$ is defined by the geometrical considerations from the relation $\sin\theta=R^*\sin(\gamma^*)/\sqrt{(R^*)^2+r^2-2R^*r\cos(\gamma^*)}$. Substituting into Eq. (16) $r=r_e/2$, $I=(m_{\mathrm{H}}/2)r_e^2$, $\mu=m_{\mathrm{H}}$, and finding $\mu^\dagger$ from the condition $\mu^\dagger=\min\{\mu_{\mathrm{EM}}(\gamma^*)\}$ at $\theta=\pi/2$, we get $\mu^\dagger/\mu=2/3=0.667$. We thus see that the fitted value of $(\mu^\dagger/\mu)_{\mathrm{P}}=0.681$ is indeed close to this simple estimate. Of course, this estimate cannot be taken too seriously; for instance, the use of $\Gamma^\dagger(\varepsilon)=\Gamma^{\mathrm{T}}(\varepsilon)$ (potential for the T configuration) would change $(\mu^\dagger/\mu)_{\mathrm{P}}=0.681$ into $(\mu^\dagger/\mu)_{\mathrm{T}}=0.745$. Note that the ratios $(\mu^\dagger/\mu)_{\mathrm{P}}=0.681$ and $(\mu^\dagger/\mu)_{\mathrm{T}}=0.745$ are noticeably lower than $(\mu^{\mathrm{eff}}/\mu)^{\mathrm{SC\text{-}BS}}=0.841$ that served as a diagnostic for the importance of rotation in inducing the vibrational transition. The reason why $(\mu^\dagger/\mu)_{\mathrm{P}}$ and $(\mu^\dagger/\mu)_{\mathrm{T}}$ are lower than $(\mu^{\mathrm{eff}}/\mu)^{\mathrm{SC\text{-}BS}}$ can be traced to the fact that the preexponential factor in the SC-OEM model, Eq. (15), introduces an extra (though weak) positive temperature dependence of the rate coefficient [as compared to the SC-BS model, Eq. (4)] thus bringing the former fitting parameter below the latter. The additional positive temperature dependence is due to the widening of the acceptance cone for optimal collisional configuration with increasing temperature.

We now turn to the consistency check for the OEM model. There are two conditions of the applicability for the optimal effective mass model: the classical character of the motion of the driving mode ensured by the classical character of the relative radial motion and the rotation of H_2 and the existence of a sharp maximum of the integrand in the three-dimensional angular counterpart of the one-dimensional angular integral in Eq. (3). We now discuss these conditions.

If the integral in Eq. (15) is calculated in the SD approximation with respect to the energy, it leads to the values which contribute most to the integral. Figure 5 shows graphs of the SD initial and final scaled energies, ε_i^* and $\varepsilon_f^*=\varepsilon_i^*+1$, for the semiclassical treatment, SD energy $\varepsilon_{\mathrm{LT}}^*$ for the common trajectory (original LT), and corrected common trajectory treatments in comparison with the mean thermal energy ε_T plotted versus temperature (upper abscissa) and reduced temperature $\varepsilon_T=T/T_{\mathrm{vib}}$ (lower abscissa). First, we notice that ε_i^* and ε_f^* converge closely to $\varepsilon_{\mathrm{LT}}^*$ only at very high temperatures, implying that the CCT approach will perform satisfactorily, say, above 2000 K (compare to Fig. 4). Second, we see that at a temperature of about 150 K, E_i^*/k is about 300 K which is noticeably higher than the characteristic rotational temperature $T_{\mathrm{rot}}=B/k=85.3$ K. We thus expect that quantum effects in the rotation of H_2 will show up below about 100 K. Experimentally, the manifestation of quantum rotation can be expected as a difference in the relaxation rates of ortho- and parahydrogen. Indeed, we see that this is substantiated by the data presented in Fig. 3.

The existence of a sharp maximum of the transition probability with respect to the angular variables, which indicates a preferable collisional configuration and very strong translational-rotational coupling near this configuration, follows from the fact that the optimal reduced mass $\mu^\dagger$ is no-

TABLE I. Relative optimal effective masses $\mu^\dagger/\mu$ for the potentials in the parallel and T-shape configurations for different dimensionality d of the SD manifolds (see text).

d	Parallel configuration	T-shape configuration
3	0.841±0.008	0.889±0.008
2	0.793±0.011	0.845±0.008
1	0.704±0.008	0.776±0.008
0	0.681±0.008	0.745±0.008

ticeably lower than μ. The ratio $(2(\mu-\mu^\dagger)/\mu)(T_{LT}/T)^{1/3}$, which appears in Eq. (9), is an important parameter that ensures a narrow range of angular integration, and, therefore, the applicability of the SD method in the angular averaging is about 4 or 5 at $T=1000$ K.

In order to see to what extent the fitting parameter $\mu^\dagger/\mu$ depends on the properties of the three-dimensional (3D) angular coordinate space effective in promoting the vibrational relaxation, we have done calculations and fittings with a modified expression in Eq. (15) for different dimensionalities d of the SD manifolds in the 3D angular space replacing the power $-3/2$ in the preexponential factor by $d/2-3/2$ ($d=0$ for a single or several SD points, $d=1$ or a one-dimensional SD manifold, $d=2$ for a two-dimensional SD manifold, and by $d=3$ for a three-dimensional manifold, the BS model). The results of the fitting are listed in Table I for P and T configurations. The deviations correspond to variations in $\mu^\dagger/\mu$ that bracket the experimental data by the respective values of $k_{10}^{\text{SC-OEM}}$. On the basis of the discussion, we believe that the dimensionality $d=0$ is the most appropriate for the H_2-H_2 collisions.

V. CONCLUSION

The Landau-Teller plot of experimental rate coefficients $k_{10}(T)$ for vibrational relaxation of H_2 in H_2 is highly nonlinear, see Fig. 4. The nonlinearity is mainly due to the large energy release ($T_{vib}\approx 6000$ K) into the heat bath which has a much lower average energy per mode ($T<3000$ K); the second reason for nonlinearity that shows up at $T<500$ K is the deviation of the interaction potential from an exponential form. The former effect is adequately described by the semiclassical approximation with a fitted value of the optimal effective mass $\mu_{OEM}=0.681$ amu and with the steepness parameter of $\alpha=1.815$ a.u. for the repulsive part of the *ab initio* potential. The latter feature is due to the shortening of the encounter time at low collision energies which results from the effective increase of the steepness of the repulsive part of the potential in the presence of an attractive well compared to a purely repulsive exponential potential (i.e., a potential with a constant steepness). The corrected common trajectory approximation with the same values for μ_{OEM} and α provides a reasonable description of experimental data only for $T>2000$ K while the simple common trajectory approach (classical heat bath) fails completely.

The fitted value of the optimal effective mass is close to that found from a simple model (in Ref. 4 characterized by the statement "the accessible repulsive core at the H atom is assumed to be of approximately spherical shape"). The noticeable deviation of the optimal effective mass from the reduced mass of the colliding partners unambiguously indicates a substantial participation of the rotation of partners in inducing the vibrational transition which is in agreement with more detailed dynamical calculations.[21–23] At the same time, the semiclassical optimal effective mass approach explains the reason for the earlier erroneous claim[20] that the breathing sphere model, which ignores the participation of rotation, satisfactorily interprets the experimental data.

Finally, we note that the given interpretation within the outlined analytical approach can also be easily applied to other interaction potentials. Then the detailed dynamical information on the energy transfer again will be hidden, such as in the present treatment, in the optimal effective mass, the reasonable value of which can hopefully be substantiated by invoking simple models.

ACKNOWLEDGMENT

The authors are indebted to D. L. Huestis for attracting their attention to the title problem and for communicating the experimental data on H_2-H_2 relaxation.

APPENDIX: GLOSSARY OF ABBREVIATIONS USED IN THIS PAPER

BS	breathing sphere
CT	common trajectory
CCT	corrected common trajectory
EM	effective mass
LT	Landau-Teller
OEM	optimal effective mass
PES	potential energy surface
SC	semiclassical
SD	steepest descent
SSH	Schwartz-Slawsky-Herzfeld

[1] G. A. Kapralova, E. E. Nikitin, and A. M. Chaikin, Chem. Phys. Lett. **2**, 581 (1968).
[2] E. E. Nikitin, *Theory of Elementary Atomic and Molecular Processes in Gases* (Clarendon, Oxford, 1974).
[3] A. Miklavc, N. Markovic, G. Nyman, V. Harb, and S. Nordholm, J. Chem. Phys. **97**, 3348 (1992).
[4] T. D. Sewell, S. Nordholm, and A. Miklavc, J. Chem. Phys. **99**, 2567 (1993).
[5] R. N. Schwartz, Z. I. Slawsky, and K. F. Herzfeld, J. Chem. Phys. **20**, 1591 (1952).
[6] R. N. Schwartz and K. F. Herzfeld, J. Chem. Phys. **22**, 767 (1954).
[7] E. E. Nikitin and J. Troe, Phys. Chem. Chem. Phys. **8**, 2012 (2006).
[8] D. Schwarzer and M. Teubner, J. Chem. Phys. **116**, 5680 (2002).
[9] M. Teubner, Phys. Rev. E **65**, 031204 (2002).
[10] E. I. Dashevskaya, I. Litvin, E. E. Nikitin, and J. Troe, J. Chem. Phys. **125**, 154315 (2006).
[11] N. Balakrishnan, R. C. Forrey, and A. Dalgarno, Phys. Rev. Lett. **80**, 3224 (1998).
[12] D. R. Flower, E. Roueff, and C. J. Zeippen, J. Phys. B **31**, 1105 (1998).
[13] N. Balakrishnan, M. Vieira, J. F. Babb, A. Dalgarno, R. C. Forrey, and S. Lepp, Astrophys. J. **524**, 1122 (1999).
[14] R. C. Forrey, V. Kharchenko, N. Balakrishnan, and A. Dalgarno, Phys. Rev. A **59**, 2146 (1999).
[15] R. C. Forrey, N. Balakrishnan, A. Dalgarno, M. R. Haggerty, and E. J. Heller, Phys. Rev. Lett. **82**, 2657 (1999).
[16] R. C. Forrey, N. Balakrishnan, A. Dalgarno, M. R. Haggerty, and E. J. Heller, Phys. Rev. A **64**, 022706 (2001).
[17] R. C. Forrey, Phys. Rev. A **63**, 051403 (2001).

[18] R. C. Forrey, Phys. Rev. A **66**, 023411 (2002).
[19] T.-G. Lee, C. Rochow, R. Martin, T. K. Clark, R. C. Forrey, N. Balakrishnan, P. C. Stancil, D. R. Schultz, A. Dalgarno, and G. J. Ferland, J. Chem. Phys. **122**, 024307 (2005).
[20] J. B. Calvert, J. Chem. Phys. **56**, 5071 (1972).
[21] R. Ramaswamy and H. Rabitz, J. Chem. Phys. **66**, 152 (1977).
[22] G. D. Billing and E. R. Fisher, Chem. Phys. **18**, 225 (1976).
[23] G. D. Billing, Chem. Phys. **20**, 35 (1977).
[24] J. H. Kiefer and R. W. Lutz, J. Chem. Phys. **44**, 668 (1966).
[25] J. E. Dove and H. Teitelbaum, Chem. Phys. **6**, 431 (1974).
[26] M. M. Audibert, R. Vilaseca, J. Lukasik, and J. Ducuing, Chem. Phys. Lett. **31**, 232 (1975).
[27] M. M. Audibert, C. Joffrin, and J. Ducuing, Chem. Phys. Lett. **25**, 158 (1974).
[28] R. G. Burton and U. E. Senff, J. Chem. Phys. **76**, 6073 (1982).
[29] G. A. Gallup, J. Chem. Phys. **66**, 2252 (1977).
[30] A. I. Boothroyd, J. E. Dove, W. J. Keogh, P. G. Martin, and M. R. Peterson, J. Chem. Phys. **95**, 4331 (1991).
[31] A. Aguado, C. Suarez, and M. Paniagua, J. Chem. Phys. **101**, 4004 (1994).
[32] T. L. Cottrell and J. C. McCoubrey, *Molecular Energy Transfer in Gases* (Butterworths, London, 1961).
[33] B. Widom, Discuss. Faraday Soc. **33**, 37 (1962).
[34] D. L. Huestis (private communication).